NeuroImage 238 (2021) 118247

Contents lists available at ScienceDirect

NeuroImage

journal homepage: www.elsevier.com/locate/neuroimage

Heartbeat and somatosensory perception

Esra Al[a,b,c,*], Fivos Iliopoulos[a,c], Vadim V. Nikulin[a,d], Arno Villringer[a,b,c]

[a] Department of Neurology, Max Planck Institute for Human Cognitive and Brain Sciences, 04103 Leipzig, Germany
[b] MindBrainBody Institute, Berlin School of Mind and Brain, Humboldt-Universität zu Berlin, 10099 Berlin, Germany
[c] Center for Stroke Research Berlin (CSB), Charité – Universitätsmedizin Berlin, 10117 Berlin, Germany
[d] Institute of Cognitive Neuroscience, National Research University Higher School of Economics, 101000 Moscow, Russia

ARTICLE INFO

Keywords:
Somatosensory processing
Perceptual awareness
Electrophysiology
Interoception

ABSTRACT

Our perception of the external world is influenced by internal bodily signals. For example, we recently showed that timing of stimulation along the cardiac cycle and spontaneous fluctuations of heartbeat-evoked potential (HEP) amplitudes influence somatosensory perception and the associated neural processing (Al et al., 2020). While cardiac phase affected detection sensitivity and late components of the somatosensory-evoked potentials (SEPs), HEP amplitudes affected detection criterion and both early and late SEP components. In a new EEG study, we investigate whether these results are replicable in a modified paradigm, which includes two succeeding temporal intervals. In one of the intervals, subjects received a weak electrical finger stimulation and reported first whether they detected any stimulation and then allocated the stimulus to one of the two intervals. Our results confirm the previously reported cardiac cycle and prestimulus HEP effects on somatosensory perception and evoked potentials. In addition, we obtained two new findings. Source analyses in this and our original study show that the increased likelihood of conscious perception goes along with HEP fluctuations in parietal and posterior cingulate regions, known to play important roles in interoceptive processes. Furthermore, HEP amplitudes were shown to decrease when subjects engaged in the somatosensory task compared to a resting state condition. Our findings are consistent with the view that HEP amplitudes are a marker of interoceptive (versus exteroceptive) attention and provide a neural underpinning for this view.

1. Introduction

Interoceptive signals from the body can influence our perception, cognition, and emotions (Critchley and Garfinkel, 2018; Garfinkel et al., 2014; Sandman et al., 1977; Saxon, 1970). For instance, different phases of the cardiac cycle (e.g., systole vs. diastole) have been reported to affect visual, auditory, and pain perception (Sandman et al., 1977; Saxon, 1970; Wilkinson et al., 2013). In the somatosensory domain, we recently demonstrated that somatosensory detection was lower during systole compared to diastole in two independent studies (Al et al., 2020; Motyka et al., 2019 but also see Edwards et al., 2009). Furthermore, our recent study (Al et al., 2020) showed that this change in detection accompanied changes in perceptual sensitivity for distinguishing the presence of stimuli from its absence, rather than in detection bias, i.e., criterion, according to signal detection theory (SDT).

Similar to the changes in perception, late components of somatosensory-evoked potentials (SEPs) and pain-evoked potentials were found to be lower during systole compared to diastole (Al et al., 2020; Gray et al., 2010). This attenuation of sensory processing during systole can be explained in an interoceptive predictive framework, which postulates repetitive bodily signals such as heartbeat-coupled events, to be predicted and suppressed from entering conscious perception. Interestingly, also perception of coincident external stimuli such as external sounds have been shown to be inhibited by these suppressive mechanisms (Van Elk et al., 2014).

Our previous study also addressed the influence of neural responses to heartbeats, known as heartbeat-evoked potentials (HEP), on somatosensory perception. Higher amplitudes of prestimulus HEP were found to be followed by lower detection rates and decreased amplitudes of early (P50) and late SEP components (N140, P300) (Al et al., 2020). The modulation of detection rates was associated with a change in detection bias but not sensitivity. Given that HEP amplitudes are higher during interoceptive compared to exteroceptive attention (García-Cordero et al., 2017; Petzschner et al., 2019; Villena-González et al., 2017), we interpreted the fluctuations of HEP amplitudes as a reflection of attentional shifts between internal bodily states and external somatosensory stimuli. Such attentional modulations of HEP amplitudes have been also proposed in response to emotional stimuli in the visual domain (Marshall et al., 2017; 2018). If HEP-related

* Corresponding author at: Department of Neurology, Max Planck Institute for Human Cognitive and Brain Sciences, 04103 Leipzig, Germany.
E-mail address: esraal@cbs.mpg.de (E. Al).

https://doi.org/10.1016/j.neuroimage.2021.118247.
Received 3 February 2021; Received in revised form 2 June 2021; Accepted 6 June 2021
Available online 7 June 2021.

modulations are connected with switches between internal and external attention, then HEP amplitudes would be expected to differ during a resting state condition compared to engaging an external task. Furthermore, such modulation of HEP is likely to occur in brain regions associated with attentional switches such as the default-mode network regions (Buckner et al., 2008; Kleckner et al., 2017).

The current study investigates heartbeat-related effects on somatosensory perception and their neural sources. In this study, we aimed to replicate and extend our previous findings (Al et al., 2020) in a different experimental setting: Since the cardiac phase effects which we observed in the yes/no detection task were weak in a forced-choice *localization* task, we now replaced the latter aspect of our paradigm with a forced-choice *detection* task (including two temporal intervals). Based on our previous findings, we hypothesized (i) a lower detection sensitivity and weaker late SEP amplitudes during systole as compared to diastole and (ii) negative relationships between HEP amplitude, the succeeding detection, and the amplitudes of early and late SEP components. Beyond the replication of our previous study, the new design allowed us (iii) to explore how detection, SEPs, and heart rate were affected depending on the stimulation interval, in which stimuli had different temporal certainties. Furthermore, we attempted to identify (iv) the neural sources of HEP differences preceding hits and misses and investigated (v) whether HEP amplitudes in general differ during a somatosensory detection task compared to a resting state condition.

2. Materials and methods

2.1. Participants

Forty healthy volunteers participated in the study. All subjects were right-handed. Four subjects were excluded from the analyses due to technical problems during the ECG data acquisition. Overall, 36 subjects (18 females, age: 25.3 ± 4.0 y [mean ± SD], range: 20 to 36 y) were included in the analyses.

2.2. Ethics statement

The study was approved by the ethics commission at the medical faculty of the University of Leipzig (no. 462–15–01062015). All participants gave informed consent and were compensated for their participation.

2.3. Somatosensory stimulation and task design

Somatosensory stimuli were presented using electrical stimulation of the finger nerve. A pair of steel wire ring electrodes was attached to the middle (anode) and the proximal (cathode) phalanx of the left index finger. Participants sat comfortably in a quiet room, with palms facing downward. Stimuli were applied using a DS-5 constant-current stimulator (Digitimer) using single square-wave pulses with a duration of 200 μs.

At the beginning of the experiment, a near-threshold stimulus intensity that could be detectable only in 50% of the trials in the yes/no detection task was determined by using a two-step procedure as described in our previous study (Al et al., 2020).

During the experiment, participants performed a combined yes/no detection and a two-interval, forced-choice, detection task (2IFC) in every trial. Each trial was separated into two temporal intervals and each interval had a duration of 1400 ms (**Fig. 1**). In stimulation trials, participants either received an electrical stimulus during the middle of the first or the second temporal interval (700 ms after the start of the interval). After the visual representation of the second interval disappeared from the screen, participants answered the question, 'Did you feel it?', as quickly as possible, by reporting 'yes' or 'no' with their right middle finger via button press. Subjects were then asked to respond to the question, 'In which temporal interval did the stimulus occur?', by choosing either '1′ with their right index finger or '2′ with their right ring finger. They were instructed 'to guess' the interval when they did not detect the presence of a stimulus in either of the intervals. Participants were told that one of the two temporal windows contained a stimulus in every trial; however, no stimulus was presented in 20 pseudorandomized trials (catch trials) out of 120 trials in every experimental block. In total, participants completed 840 trials over 7 blocks. Each block lasted for ~10 min. After each block, stimulation intensities were readjusted to a threshold level.

2.4. Data and code availability

Data and code will be available upon request. Due to a lack of explicit consent on the part of the participants to data sharing, structural MRI and EEG data cannot be shared publicly. Such data can only be shared upon request if data privacy can be guaranteed according to the rules of the European General Data Protection Regulation (EU GDPR).

2.5. Cardiac cycle analyses

The changes in somatosensory detection were evaluated across the two phases of the cardiac activity: systole and diastole. Systole was operationalized as 'the time between the R-peak and the end of the t-wave' (Motyka et al., 2019; Al et al., 2020). This systolic window length was then used to define a 'diastolic window of equal length at the end of each cardiac cycle' (Al et al., 2020). By defining equal lengths of systole and diastole, we balanced the probability of stimulation during the phases (Al et al., 2020). For each cardiac cycle, we used a trapezoid area algorithm to determine the end of the t-wave (Al et al., 2020; Motyka et al., 2019; Vázquez-Seisdedos et al., 2011). As a result, the average systole (and diastole) length was 338±24 ms.

2.6. EEG and ECG recordings

EEG data were recorded from 62 electrodes (61 scalp electrodes plus 1 electrode recording the VEOG below the right eye), using a commercial EEG acquisition system (actiCap, BrainAmp; Brain Products) with a bandwidth of 0.015–1000 Hz and a sampling rate of 2500 Hz. The following scalp electrodes were used according to the international 10–10 system: FP1, FP2, F7, F3, Fz, F4, F8, FC5, FC1, FC2, FC6, T7, C3, Cz, C4, T8, CP5, CP1, CP2, CP6, AFz, P7, P3, Pz, P4, P8, PO9, O1, Oz, O2, PO10, AF7, AF3, AF4, AF8, F5, F1, F2, F6, FT7, FC3, FC4, FT8, C5, C1, C2, C6, TP7, CP3, CPz, CP4, TP8, P5, P1, P2, P6, PO7, PO3, POz, PO4, PO8. During the measurement, the EEG signal was referenced to FCz while an electrode on the sternum served as ground. Electrode impedance was kept ≤5 kΩ for all channels. The position of the individual electrodes was measured in 3D space for each subject using a Patriot motion tracker (Polhemus). To record heart activity, an ECG electrode was mounted under the left breast of the subjects. EEG and ECG data were first acquired during two 4-min eyes-closed resting-state conditions and then during the somatosensory task.

2.7. Data preprocessing

EEG data were preprocessed using EEGLAB (Delorme and Makeig, 2004) and custom-written scripts in MATLAB (MathWorks Inc.). A low-pass finite impulse response filter (112.5 Hz) was applied before downsampling EEG data to 250 Hz. All experimental blocks were concatenated and then passed through first a high- and then a low-pass filter (0.3–45 Hz) using the fourth order Butterworth filter. The noisy EEG channels with a flat line longer than 5 s or a correlation less than 85% with their reconstructed activity from the rest of the channels were removed. Then, their activity was interpolated from their neighboring channels (using "clean_rawdata" plug-in of EEGLAB). After application of principal component analysis, an independent component analysis (ICA) was performed using an extended infomax algorithm to remove

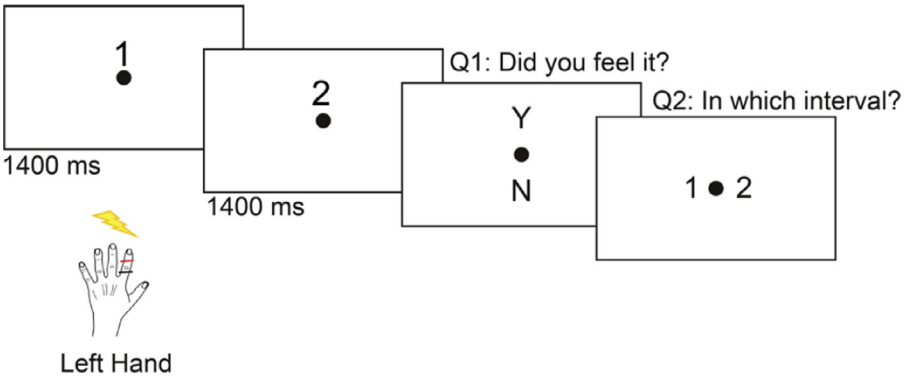

Fig. 1. Experimental paradigm. Thirty-six participants received a weak electrical pulse to the left index finger in 720 out of 840 trials over seven experimental blocks. Participants were told that one of the two temporal windows in every trial contained a stimulus; however, no stimulus was actually presented in 120 pseudorandomized trials. In every trial, participants performed a combined yes/no detection and a two-alternative forced choice task.

the ocular and heartbeat artifacts (Delorme et al., 2012). To specifically remove the heartbeat-related artefactual ICA components, the ECG R-peak positions were first identified using the HEPLAB toolbox, which was followed by a visual correction (Perakakis, 2019). ICA data were then copied and epoched according to R-peak position (−100–800 ms) to ease the selection of the heartbeat artifacts that show a similar time-course with the R-peak and t-wave of the ECG activity. Artefactual independent components were then visualized using the SASICA software (Chaumon et al., 2015) and selected manually for rejection. After removal of the artefactual ICA components, the continuous artifact-free components were forward projected. EEG data were then re-referenced to an average reference.

2.8. Somatosensory-Evoked potential (SEP) analyses

EEG data were epoched between −1000 to 2000 ms around the stimulus onset individually for trials with stimulation during systole and diastole. A baseline correction was done using the −100–0 ms window. The calculation of 'maximum positive deflection of the early SEP component P50 (40–60 ms)' (Al et al., 2020; Nierhaus et al., 2015; Zhang and Ding, 2010) suggested the C6 electrode as the representative electrode of the contralateral primary somatosensory area. Since the representative electrode was determined as C4 in our previous study (Al et al., 2020), we selected a cluster of electrodes neighboring the C6 electrode (C4, CP4, C6, CP6) broadly covering brain structures relating to somatosensory processing. Statistical analyses of SEP amplitudes were performed on these 4 electrodes. Following our previous study, we also estimated and cleaned artefactual effects of blood circulation on the EEG data (see Al et al., 2020 for details of the ECG-induced artifact cleaning on the SEPs).

2.9. Heartbeat-Evoked potential (HEP) analyses

In our analysis of HEP, we selected the trials where the somatosensory stimulation occurred at least 400 ms after the preceding R-peak (corresponding to diastole) to ensure that the time window for neural responses to heartbeats was not contaminated by stimulation-related activity (Al et al., 2020). As a result of this selection, on average 472±44 trials per subject were included to determine HEPs by segmenting data around the R-peak. This allowed us to evaluate prestimulus HEPs, often reported between 250 and 400 ms after the R-peak (Kern et al., 2013; Schandry et al., 1986; Schandry and Weitkunat, 1990).

2.10. Source reconstruction analyses

The neural sources of the EEG signal were reconstructed on the BrainStorm toolbox (Tadel et al., 2011) using individually measured electrode positions (in 29 subjects). Standard electrode positions were used for 7 subjects since some problems were identified in their recorded electrode positions. When available, individual brain anatomies (17 subjects) and otherwise a template brain anatomy (ICBM152; (Fonov et al., 2009) were used. The structural T1-weighted MRI images were segmented using Freesurfer (http://surfer.nmr.mgh.harvard.edu/). A 3-shell boundary element model (BEM) was constructed to compute the lead field matrix with OpenMEEG (Gramfort et al., 2010; Kybic et al., 2005). The lead field matrices were inverted using eLORETA separately for each condition and subject. The Matlab code for eLORETA was derived from the MEG/EEG Toolbox of Hamburg (METH). Individual source data were then baseline-normalized with −100 to 0 ms time-window and projected to the ICBM152 template. The segmentation of the cortical anatomy was performed according to the Destrieux atlas (Destrieux et al., 2010).

2.11. Signal detection theory (SDT) analyses

In the presence of a stimulus, a trial was categorized as a hit if subjects reported detecting it and as a miss if they reported not feeling it. A false alarm (FA) occurred when subjects reported detecting a stimulus in its absence in the yes/no detection task. Using the hit and FA rates we calculated signal detection theory measures to differentiate sensitivity (d') and criterion effects in the yes/no detection task (Al et al., 2020).

2.12. Statistical analyses

As described in our previous study, we statistically tested the two-condition comparisons of EEG data using cluster-based permutation t-tests in the FieldTrip toolbox (Oostenveld et al., 2011). For comparison of the conditions regarding the sensory-level SEP activity, cluster statistics were conducted over a set of somatosensory electrodes (C4, CP4, C6, CP6) either for the mean activity across the previously identified time window of 268–468 ms or for the whole time window of 0–600 ms. For comparison of HEP activity preceding hits and misses, we tested mean differences between 296 and 400 ms over a cluster of electrodes (FC2, Cz, C4, CP1, CP2, Pz, P4, C1, C2, CPz, CP4, P1, P2) as in our previous study (Al et al., 2020). This analysis was also performed to compare HEP differences during the resting state and task. The behavior across the HEP bins were tested by using repeated measures correlation coefficient by using 'rmcorr' function in Rstudio (v 1.3.1093).

For the statistical test of the neural sources of differential HEP amplitudes, we used cluster statistics. Mean HEP amplitude between 296 and 400 ms following the R-peak were compared between hits and misses in a dataset of 37 subjects from our previous study (Al et al., 2020) over 15,000 cortical vertices. The resulting cortical regions were used as the regions of interest for the HEP analyses in the present dataset.

The cardiac phase effects on yes/no and 2IFC detection were done using within-subject ANOVAs by using the ezANOVA function in Rstudio. Detection rates were analyzed as dependent variables in within-subject ANOVA tests in which stimulation interval and cardiac phase were in-

dependent variables. Intervals were included as a factor here since an effect of stimulation interval on detection rates was expected and we aimed to test possible interaction effects between the cardiac phase and the intervals. For the calculation of SDT parameters across the cardiac cycle, we only tested the phase effects by using within-subject *t*-tests similar to our previous study. Since false alarm rates were very low in our experiments, the interval was not used as a factor here since this would further lower the number of false alarms for every condition, which can create unreliable estimations of sensitivity and criterion.

For the within-subject ANOVAs, violations of the sphericity assumption were corrected with the Greenhouse–Geisser method. All statistical tests were two-sided.

3. Results

Thirty-six participants were presented weak somatosensory stimuli (electrical) to the left index finger in a combined yes/no and 2IFC detection task (**Fig. 1**). Both EEG and electrocardiography (ECG) were recorded. On average, participants detected 52.2 ± 10.0% (mean ± SD) of the somatosensory stimuli with a false alarm rate of 8.6 ± 11.4%. Participants correctly detected 79.4 ± 5.6% of the stimulation intervals.

3.1. Somatosensory perception changes across the cardiac cycle

We first tested the hypothesis that somatosensory detection is less likely during cardiac systole compared to diastole, as found in our previous studies (Al et al., 2020; Motyka et al., 2019). For this purpose, we determined when stimulus onsets occurred during systole and diastole. Then, a within-subject ANOVA test was applied to investigate the effect of stimulation interval and cardiac phase on detection rates. As expected, detection rates were higher during diastole ($F_{1,35}$=11.42, $p = 2{\cdot}10^{-3}$). Also, stimuli during the second temporal interval were detected more often ($F_{1,35}$=27.60, $p = 7{\cdot}10^{-6}$). We did not observe a significant interaction between the temporal interval and cardiac phase ($F_{1,35}$=0.99, p = 0.3; **Fig. 2a**). Furthermore, the effect of cardiac phase on 2IFC detection was tested. A within subject ANOVA showed that neither cardiac phase ($F_{1,35}$=1.57, p = 0.2) nor stimulation interval ($F_{1,35}$=1.10, p = 0.3) had a significant effect on 2IFC detection.

Of 36 participants, 27 had a lower yes/no detection rate during systole. We furthermore checked whether this cardiac phase effect on detection was correlated with individual differences in the heart rate or heart rate variability (HRV, i.e., the standard deviation of RR intervals). Based on our previous results, a significant correlation with HRV was expected (Al et al., 2020). However, subjects' detection rate difference between the two cardiac phases did not significantly correlate with either their heart rate or HRV (respectively, Pearson's correlation, r=−0.05, p = 0.77 and r = 0.21, p = 0.22).

Next, we tested whether the changes in the yes/no detection rates were associated with changes in perceptual sensitivity (*d'*) according to Signal Detection Theory (SDT). Confirming our previous finding, detection sensitivity was found to be significantly lower during systole (M = 1.43) relative to diastole (M = 1.75), t_{35}=−3.77, $p = 6{\cdot}10^{-4}$ (**Supp. Fig. 1a**). For the criterion, we observed a trend between systole (M = 0.71) and diastole (M = 0.79), t_{35}=−1.95, p = 0.06 (**Supp. Fig. 1b**).

Somatosensory detection rate was previously shown to be lowest when stimulation occurred 200–400 ms after the previous heartbeat (Al et al., 2020). To test the reliability of this result, we tested the effect of the time delay of somatosensory stimulation from the previous R-peak on yes/no detection performances. Within-subject ANOVAs confirmed that detection performance significantly differed between four time-windows: 0–200, 200–400, 400–600, and 600–800 ms ($F_{3,105}$=9.58, $p = 1{\cdot}10^{-5}$). Also, a trend for 2IFC detection was observed ($F_{3,105}$=2.36, p = 0.07). *Post-hoc* paired *t*-tests between 0 and 200 and 200–400 ms and 200–400 and 600–800 ms revealed that yes/no detection was lowest 200–400 ms after the R-peak (t_{35}=3.32, p = 0.002 and t_{35}=−4.22, $p = 2{\cdot}10^{-4}$, **Fig. 2**).

3.2. Somatosensory-evoked potentials change across the cardiac cycle

Similar to perceptual attenuation, the amplitude of the P300, a late component of somatosensory-evoked potentials (SEPs), has also been previously reported to decrease during systole. Therefore, we expected to observe decreased P300 activity in response to stimulation during systole compared to diastole. To test this hypothesis, we first checked the mean P300 difference in the time window of 268–468 ms, as previously reported, between systole and diastole over the contralateral somatosensory cortex (indexed by C4, C6, CP4, CP6). The cluster statistics testing the mean SEPs between 268 and 468 ms over the somatosensory electrodes showed only a trend effect, suggesting a lower mean P300 activity during systole compared to diastole (Monte Carlo p = 0.07, corrected for multiple comparisons in space). The changes in the mean P300 activity were also tested across four time bins depending on the distance of stimulation from the previous R-peak: 0–200, 200–400, 400–600, and 600–800 ms. Again, a trend for the mean P300 amplitude was observed ($F_{3,105}$=2.40, p = 0.07, **Supp. Fig. 2**).

We then performed a cluster-based permutation *t*-test comparing SEPs during the two cardiac phases between 0 and 600 ms following stimulus onsets, over the contralateral somatosensory cortex. The results showed that during a later time window (512–600 ms) following stimulation, during systole, late SEPs showed decreased positivity (Monte Carlo p = 0.02, corrected for multiple comparisons in time and the region of interest electrodes; **Fig. 3a**). To confirm that the SEP differences across the cardiac cycle originate from the contralateral somatosensory cortex (S1), we also performed a source reconstruction analysis (**Fig. 2d**). Source analysis confirmed that late P300 amplitude in S1 was significantly different between the two cardiac phases (t_{35}=−2.78, p = 0.01; **Fig 2d**).

We additionally checked SEP amplitudes separately for stimulations presented in the 1st and 2nd temporal intervals during systole and diastole over S1 at the sensory (**Fig 2e**) and source level (**Fig 2f**). Subjects showed a higher mean P300 response (between 512 and 600 ms across the somatosensory electrodes) to stimuli during the second compared to the first temporal interval (t_{35}=−5.78, $p = 2{\cdot}10^{-6}$). To test a possible interaction effect between the interval and cardiac phase, we calculated the difference of P300 amplitudes between systolic and diastolic stimuli presented during the first and second interval. This analysis did not reveal any significant interaction effect (t_{35}=0.94, p = 0.4).

3.3. Heart rate and the stimulation interval

When a stimulus is not presented in the first but the second interval, then subjects have an increased expectancy for the stimulus. We investigated whether changes in the stimulation expectancy in the two temporal intervals were associated with the changes in the heart rate before and after stimulation (S-1, S, $S+1$, $S+2$). The analysis showed the main effect of time ($F_{2.18,\ 76.13}$=22.04, $p = 1{\cdot}10^{-8}$) and interval ($F_{1,\ 36}$=46.55, $p = 1{\cdot}10^{-7}$) as well as their interaction ($F_{2.00,\ 70.06}$=37.42, $p = 1{\cdot}10^{-11}$) on heart rate (**Supp. Fig. 3a**).

To further explore the relationship between heart rate change and stimulation interval, the "slopes" of the stimulus-induced heartbeat changes (*Stimulus – S-1*) were compared between the two temporal intervals. While a somatosensory stimulus in the second interval was accompanied by a cardiac deceleration (M = 22.48), a stimulation during the first interval was associated with a cardiac acceleration (M = −16.99, t_{35}=−8.93, $p = 2{\cdot}10^{-9}$, **Supp. Fig. 3b**). Since the prestimulus interval was brief in our experiment, this acceleration might be related to the post-stimulation effects (particularly associated with the motor response) from the previous trial.

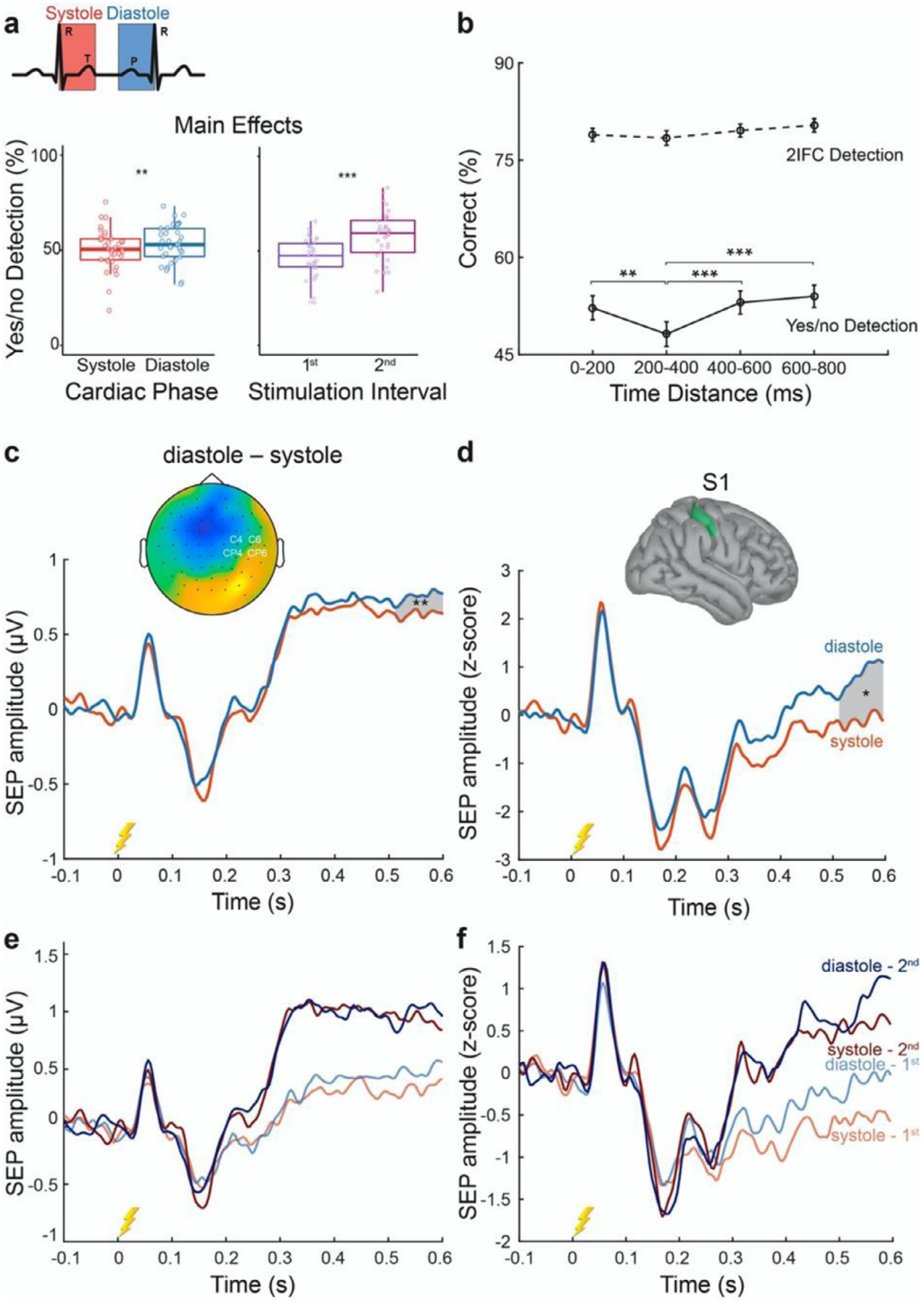

Fig. 2. Somatosensory perception and evoked potentials across the cardiac cycle. (a) The effect of stimulation interval and cardiac phase on correct detection of stimulus presence (yes/no). When a stimulus coincided with systole compared to diastole, participants detected its presence less often ($F_{1,35}$=11.42, $p = 2{\cdot}10^{-3}$). Similarly, detection rates increased during the second compared to first stimulation interval ($F_{1,35}$=27.60, $p = 7{\cdot}10^{-6}$). No significant interaction effect between the interval and cardiac phase was observed ($p = 0.3$). (b) Correct yes/no and 2IFC detection of somatosensory stimuli relative to their distance from the previous R-peak. Yes/no detection performance was lowest 200–400 ms after the R-peak (*post-hoc* paired *t*-test between 200 and 400 and 600–800 ms, t_{35}=−4.22, $p = 2{\cdot}10^{-4}$). (c) Grand average somatosensory-evoked potentials (SEPs) for electrical stimulations during systole and diastole. The P300 component of SEPs was less positive for stimuli during systole than diastole between 512 and 600 ms after stimulus onset at a cluster of electrodes (indicated with the white text) around the contralateral somatosensory cortex (Monte Carlo $p = 0.004$). The topography plot shows the contrast between diastole and systole between 512 and 600 ms. (d) The source-reconstructed P300 amplitude was significantly different between systole and diastole in the contralateral somatosensory cortex (S1) similar to the sensory data (t_{35}=−2.78, $p = 0.01$). (e-f) SEP amplitudes separately for stimulations presented in the 1st and 2nd temporal intervals during systole and diastole in (e) sensory and (f) source level. Error bars represent SEMs. $^{*}p<0.05$, $^{**}p<0.005$, $^{***}p<0.0005$, ns, not significant.

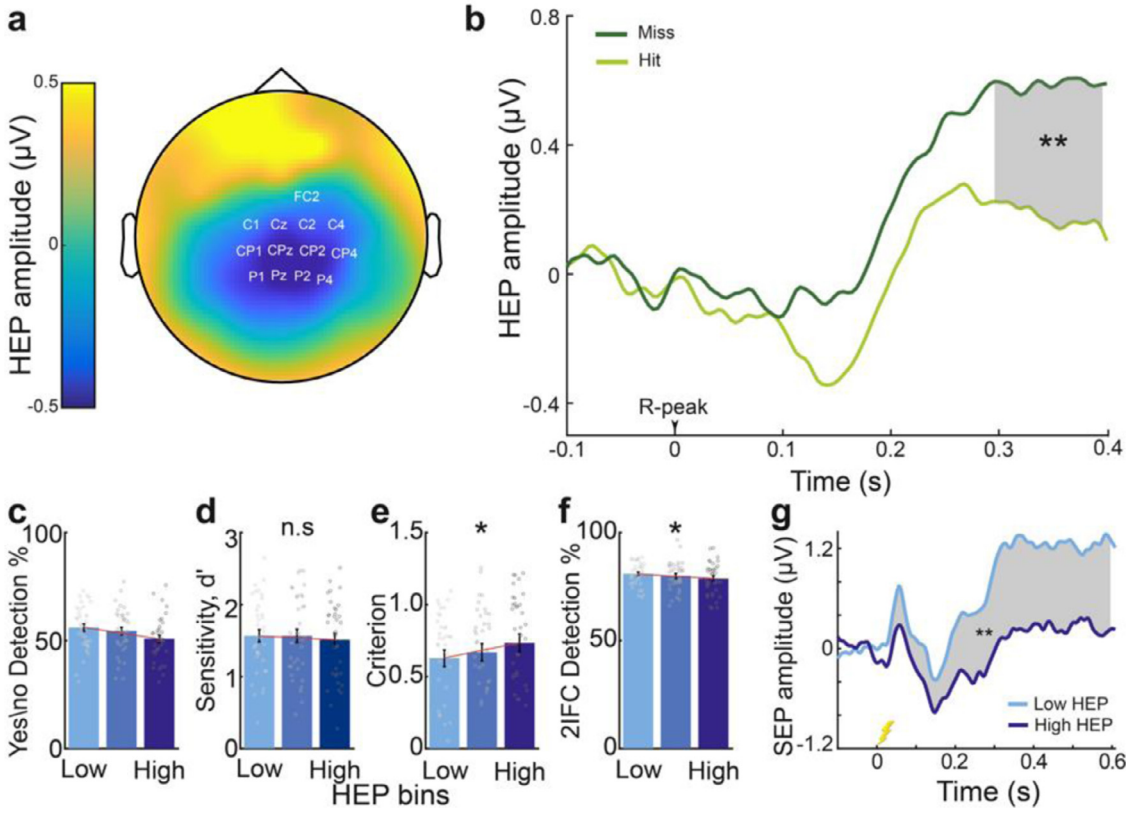

Fig. 3. The effect of prestimulus HEPs on the upcoming somatosensory perception. (a) The topography contrast of prestimulus HEP amplitude preceding hits and misses between 296 and 400 ms following the R-peak. The region of interest electrodes that were used in the HEP analyses are highlighted. (b) In 36 participants, mean HEP amplitudes between 296 and 400 ms were higher preceding misses than hits across the centroparietal electrodes (Monte Carlo $p = 0.001$) (c-f). For every trial, the mean HEP amplitude was calculated across the indicated electrodes in the 296 to 400 ms time window. Then, single trials were sorted depending on the mean HEP amplitude and divided into three equal bins for each participant. (c) Yes/no detection rate decreased as HEP amplitude increased. (d) This change in detection of stimulus presence was not correlated with a significant decrease in sensitivity ($p = 0.45$), (e) however it was connected with an increase in detection criterion, i.e., having a more conservative decision bias ($p = 0.01$). (f) Similarly, the correct allocation of stimulus into its temporal interval decreased as HEP amplitudes increased ($p = 0.01$). The individual participant data are shown on the bar plots as gray points. (g) SEP amplitudes following low and high HEP amplitudes. Following lower HEP amplitudes, mean SEPs between 32 and 600 ms following stimulation were significantly more positive over contralateral somatosensory electrodes (C4, CP4, C6, CP6; Monte Carlo p= 0.001). Error bars represent SEMs. $^{*}p<0.05$, $^{**}p<0.005$; n.s., not significant.

3.4. Heartbeat-evoked potentials negatively correlate with upcoming somatosensory detection and evoked-potentials

Following our previous study, we hypothesized that HEPs preceding stimulus onset predict somatosensory detection. More specifically, we expected to observe higher HEP amplitudes preceding misses compared to hits, across the centroparietal electrodes (FC2, Cz, C4, CP1, CP2, Pz, P4, C1, C2, CPz, CP4, P1, P2) as reported by Al et al. (2020). In the present study, prestimulus mean HEPs between 296 and 400 ms following the R-peak were again found to be higher before misses than hits over the centroparietal electrodes (Monte Carlo $p = 0.001$, corrected for multiple comparisons across the region of interest electrodes; **Fig. 3a**). We furthermore confirmed the prestimulus HEP differences between hits and misses separately for stimulations during the first and second temporal intervals (**Supp. Fig. 4**).

Because of our previous results, we expected this HEP difference to be reflected in a change in criterion (detection bias) rather than sensitivity, in the SDT framework. To test this hypothesis, we sorted single trials according to mean HEP amplitude (across the centroparietal electrodes in the 296–400 ms time window) and split them into three equal bins for each participant. Again, we found that decrease in detection with increasing HEP amplitudes was paralleled by an increase in detection criterion (Repeated measures correlation, $r = 0.29$, $p = 0.01$, **Fig. 3e**). In other words, when HEP levels were higher, participants were more conservative in reporting that they felt a stimulus. No significant changes were observed in sensitivity over HEP bins ($r=-0.09$, $p = 0.45$, **Fig. 3d**). We then tested whether prestimulus HEP amplitude also affected subject's ability to correctly detect the temporal interval of the stimulation. Similar to yes/no detection, 2IFC detection decreased as HEP levels increased ($r=-0.30$, $p = 0.01$, **Fig. 3f**).

We furthermore tested the effect of prestimulus HEP amplitude on the subsequent SEP amplitude. Given our previous results, we expected that following lower HEP amplitude, the upcoming SEPs in the time window of 32–600 ms (0=stimulus onset) would have higher positivity. Confirming our previous findings, SEPs following low, compared to high amplitude HEPs, were observed to have higher positivity between 32 and 600 ms after stimulation over the somatosensory electrodes (Monte-Carlo $p = 0.001$; **Fig. 3g**). The source analysis also confirmed that following low and high HEP levels, the amplitude of the P50, an early SEP component, was significantly different over S1 ($t_{35}=2.40$, $p = 0.02$). In our previous study this P50 modulation was also observed in other brain areas known to play a role in heart-brain interactions, such as the right anterior insula and bilateral posterior cingulate and lateral prefrontal cortices (PCC, LPFC). Thus, we again tested for P50 differences in those areas. Similarly, following low and high HEP levels, P50 amplitudes were found to be significantly different (after false discovery rate correction, $p<0.01$) in the right anterior insula ($t_{35}=2.98$, $p = 0.005$), the left and right PCC ($t_{35}=-5.77$ $p = 2{\cdot}10^{-6}$ and $t_{35}=-6.23$, $p = 4{\cdot}10^{-7}$), and the left LPFC ($t_{35}=-2.77$, $p = 0.009$). Only a trend was observed in the right LPFC ($t_{35}=-2.63$, $p = 0.01$).

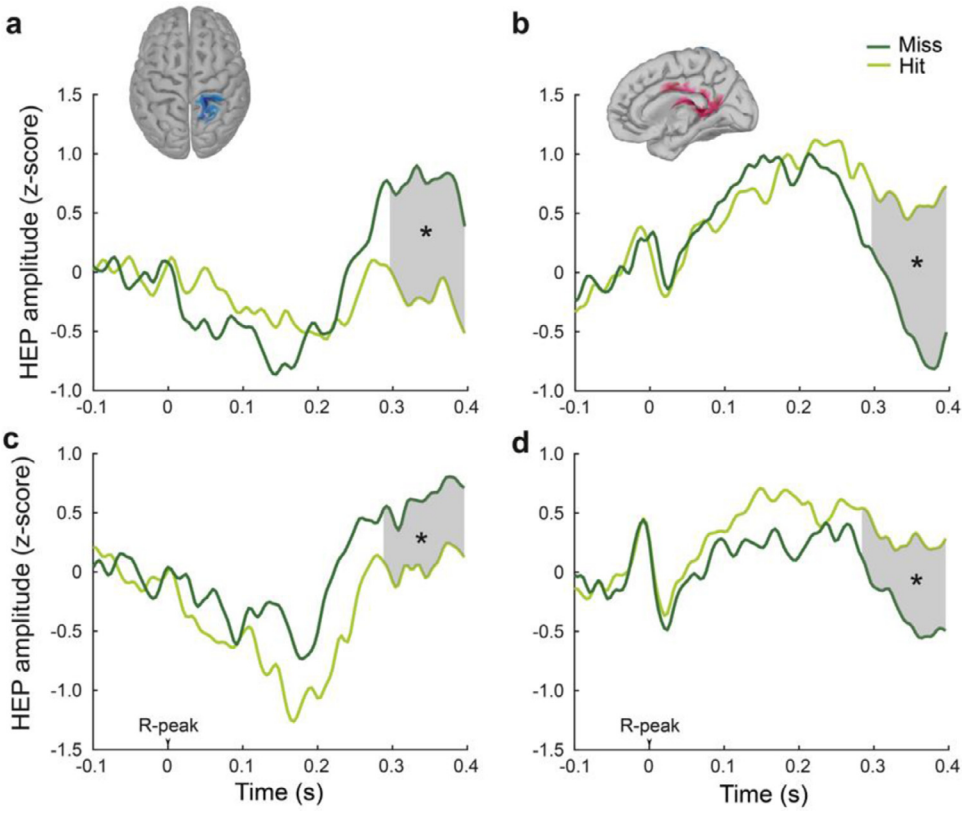

Fig. 4. Neural sources of the differential heartbeat-evoked potentials (HEPs) preceding detection. (**a-b**) The neural sources of HEP differences preceding hits and misses were determined in a previous EEG dataset with 37 subjects from the study of Al et al. (2020). Cluster statistics comparing mean HEP amplitudes between 296 and 400 ms following the R-peak across all cortical vertices for hits and misses revealed two clusters: (**a**) one extending from the postcentral gyrus and sulcus, the paracentral lobule and sulcus to the superior parietal lobule (Monte Carlo p = 0.02 corrected for multiple comparisons in space and time) and (**b**) another extending across the precuneus, isthmus of the cingulate, middle and posterior cingulate cortex, and the pericallosal sulcus (Monte Carlo p = 0.02). (**c-d**) In the present study, mean HEP amplitudes (between 296 and 400 ms) preceding hits and misses were significantly different over (**c**) the parietal regions (indicated with blue in the cortex, t_{35}=−2.44, p = 0.02 and (**d**) the posterior cingulate areas (indicated as red, t_{35}=2.86, p = 0.01), confirming HEP differences from the first dataset. *p<0.05.

In an exploratory analysis, we also tested overall changes in HEP levels preceding hits and misses across all electrodes for the entire window of HEP, 296–400 ms after the R-peak. A cluster-based permutation *t*-test revealed a significant positive cluster over frontal electrodes and a negative cluster over centroparietal electrodes between 296 and 400 ms (Monte-Carlo p = 0.002 and p = 0.001 corrected for multiple comparisons in space and time; **Supp. Fig. 5).** The significant result, including a negative cluster over centroparietal electrodes, replicated our hypothesis-driven analyses, where misses were preceded by higher positivity of HEP. The frontal regions in the positive cluster had a negative HEP polarity and the absolute strength of prestimulus HEP for misses was similarly higher than hits. Since there were no significant differences in ECG amplitude preceding hits and misses (no clusters were found), the HEP differences in neural data cannot be explained by volume conduction of cardiac electrical activity.

3.5. Neural sources of the differential heartbeat-evoked potentials

To reveal the cortical regions contributing to the differential responses to prestimulus heartbeats in hits and misses, we first ran source reconstruction analysis on the EEG dataset from our previous study (Al et al., 2020). The cluster statistics contrasting mean HEP amplitudes between 296 and 400 ms across all cortical vertices between hits and misses showed that two regions in the right hemisphere were differentially activated. The first extended from the postcentral gyrus/sulcus and the paracentral lobule/sulcus to the superior parietal lobule (Monte Carlo p = 0.02, **Fig. 4a**). The other extended across the precuneus, isthmus of the cingulate, middle and posterior cingulate cortex, and the pericallosal sulcus (Monte Carlo p = 0.02, **Fig. 4b**). These two regions of interest were used to test mean HEP differences preceding hits and misses in our current study. Our analyses confirmed the differential mean HEP activity between 296 and 400 ms in both regions (the parietal areas: t_{35}=−2.44, p = 0.02, **Fig. 4c** and the cingulate areas: t_{35}=2.86, p = 0.01, **Fig. 4d**).

3.6. Heartbeat-evoked potentials decrease during a somatosensory task compared to a resting-state condition

If HEP amplitudes decrease as a result of externally oriented attention, then HEP levels would be expected to be lower during a somatosensory task compared to a resting-state condition. To test this hypothesis we contrasted HEP amplitudes from a resting-state condition with HEP amplitudes preceding stimuli during the somatosensory task. Cluster statistics comparing mean HEP amplitudes between 296 and 400 ms following the R-peak confirmed that HEP amplitudes were lower during the task compared to a resting-state condition over the centroparietal electrodes (Monte-Carlo p = 0.01 corrected for multiple comparisons in space, **Fig. 5a**). We furthermore compared heart rate during the resting state and the task. No significant differences in heart rate were found (t_{35}=0.63, p = 0.53).

We then compared mean HEP amplitudes during the resting state with those preceding hits and misses (indicated in **Fig. 5b**). HEPs during rest were higher than those preceding hits (t_{35}=4.12, p = $2{\cdot}10^{-4}$) but not misses (t_{35}=−0.04, p = 0.97). Source-reconstructed HEP amplitudes during rest were then contrasted with those preceding hits and misses over the parietal and cingulate areas, as these regions were determined in the previous section (see *3.4* for details). In the parietal areas, mean HEPs between 296 and 400 ms during the resting-state were significantly different from those preceding hits (t_{35}=3.03, p = $4{\cdot}10^{-3}$) and showed a trend against misses (t_{35}=2.03, p = 0.05; **Fig. 5c**). In the posterior cingulate areas, mean HEP amplitudes during rest were again significantly different than those preceding hits (t_{35}=−2.13, p = 0.04) but not misses (t_{35}=0.11, p = 0.91; **Fig. 5d**).

4. Discussion

The findings of our study replicate the effect of stimulus timing during the cardiac cycle and prestimulus HEP amplitudes on somatosensory perception and evoked potentials. Somatosensory detection was again

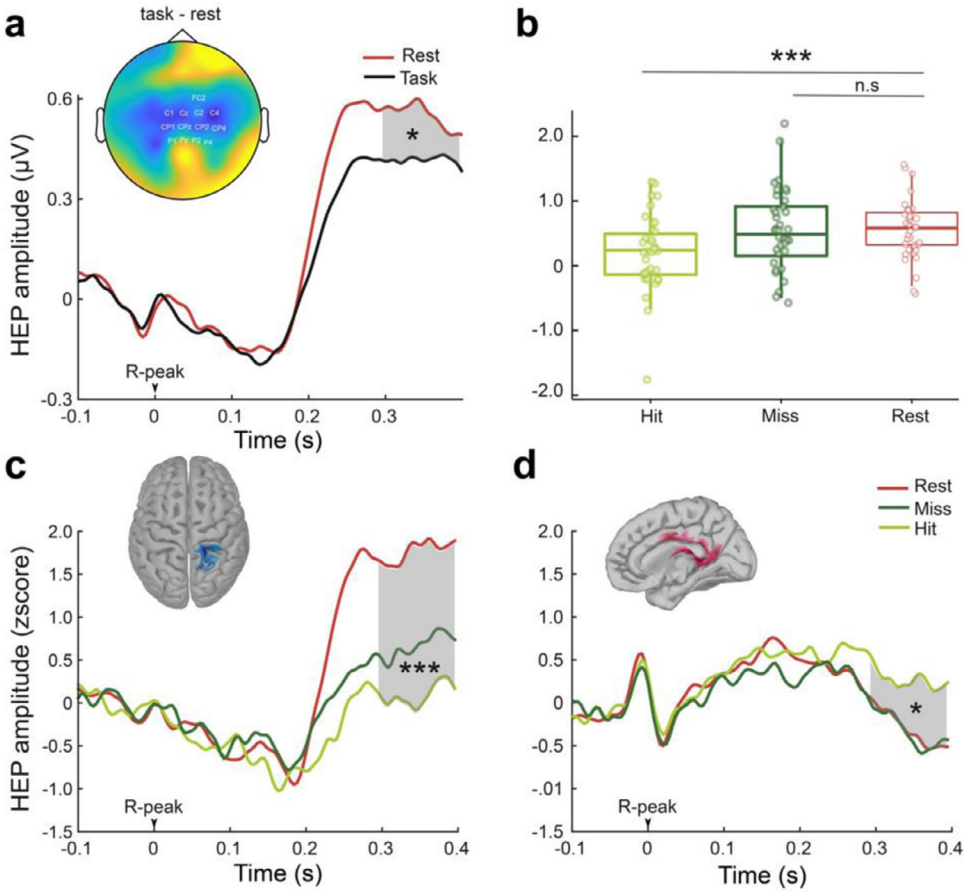

Fig. 5. HEP amplitudes during a somatosensory task compared to a resting-state condition. (**a**) HEP amplitudes over a cluster of centroparietal electrodes (indicated with the white text on the topoplot) between 296 and 400 ms were lower during the task compared to a resting-state condition (Monte-Carlo p = 0.01 corrected for multiple comparisons in space). (**b**) Mean HEP amplitudes (across the indicated cluster electrodes between 296 and 400 ms) during the resting state were compared with HEP amplitudes preceding hits and misses. During the resting-state condition, HEP amplitudes were higher than those preceding hits (t_{35}=4.12, $p = 2{\cdot}10^{-4}$) but not misses (t_{35}=−0.04, $p = 0.97$). (**c**) Source-reconstructed HEP activity during a resting-state condition and before detecting or missing a somatosensory stimulus are shown in the parietal regions extending from the postcentral gyrus and sulcus and the paracentral lobule and sulcus to the superior parietal lobule. In the parietal areas, HEPs during the resting-state significantly differed from those preceding hits (t_{35}=3.03, $p = 4{\cdot}10^{-3}$) and showed a trend compared to misses (t_{35}=2.03, p = 0.05). (**d**) In the predefined regions around the cingulate areas (indicated with red), HEP amplitudes during rest were again significantly different than those preceding hits (t_{35}=−2.13, $p = 0.04$). In this region, no significant differences were found between resting-state HEPs in comparison to those before misses (t_{35}=0.11, $p = 0.91$). $^{*}p<0.05$, $^{**}p<0.005$, $^{***}p<0.0005$, ns, not significant.

found to be lower during systole compared to diastole and to correlate negatively with prestimulus HEP amplitudes. Consistently, the cardiac phase effect on detection was associated with changes in detection sensitivity, whereas the HEP effect correlated with criterion. Moreover, the cardiac phase was again found to affect only late SEP components, while prestimulus HEP amplitudes influenced both early and later components. The new source analyses, on two different datasets, shows that HEP modulations specifically in the right posterior cingulate and parietal areas were related to changes in somatosensory perception. Subjects' HEP amplitudes, preceding misses during the somatosensory task, were also shown to approach the level during the resting-state, when exteroceptive attention is expected to reach a minimum.

We previously interpreted the changes in the detection and neural responses across the cardiac cycle in an interoceptive predictive coding framework. In this framework, rhythmic bodily fluctuations such as the heartbeat are treated as predictable events and the resulting physiological changes in the body are suppressed from being consciously perceived. In this way, the brain can minimize interference from self-generated signals such as heartbeat-related firing changes (Barrett and Simmons, 2015; Seth and Friston, 2016). For example, afferent neurons in the fingers have been shown to fire in response to the changes in the pressure wave, which can be predicted and suppressed by the central processes (Macefield, 2003). Since the pulse wave transit time is generally stable at least for certain conditions (e.g., sitting vs lying), these "stable predictions" can be assumed to be stored in the brain. Thus, pulse-related "noise" does not have to be "calculated" for each heartbeat but rather the predictive model is applied according to the respective condition. It seems plausible that the brain is quickly informed about each heartbeat (e.g., through baroreceptor activity) and accordingly expects pulse-related noise/activity in the time window of pulse arrival in the periphery. During this phase, it is likely that the perception of a weak somatosensory stimulus could be also suppressed with other heartbeat-related signals. In our current study, stimulus detection was again observed to be minimal when stimuli were presented 200–400 ms following the heartbeat (R-peak), roughly coinciding with the pulse-wave. Therefore, our new findings support the predictive mechanisms as described above.

While we previously reported that the suppression of somatosensory stimuli correlated with heart rate variability of the subjects (Al et al., 2020), we could not replicate this finding in the current study. This difference might be due to the different stimulation paradigm which involves less temporal certainty about the stimulation. Given the diverging findings, however, presently it is not clear whether a stable prediction of the timing of the "next heartbeat" plays a role in the proposed predictive (suppressive) mechanisms or whether the latter entirely rely on the rapid application of stored predictive models of pulse-related effects within each cardiac cycle (as we propose). Future studies in larger cohorts might clarify any potential role of HRV.

Similar to our previous results (Al et al., 2020), we found that the decrease in yes/no detection rates was reflected in a decrease in detection sensitivity. In other words, during systole, participants were worse at distinguishing the presence of the weak somatosensory stimuli from the internal noise. Interestingly, even though we observed significant modulation of yes/no detection rates along the cardiac cycle, we did not observe significant changes in the subjects' ability to allocate a stimulus into the correct temporal interval in a two-interval forced-choice (2IFC) detection task. A major difference between the yes/no versus 2IFC task is the subjects' far better performance in the 2IFC task, i.e., in many trials in which the subjects responded "no" for stimulus detection they nevertheless chose the right interval. We assume that in these cases, in which the stimulation was perceived "below the criterion for saying yes", there was still some information in the brain to correctly allocate

the stimulation interval. In other words, it seems that – despite of not reaching the threshold for conscious experience - the "suppressed" information still allows for a correct decision. A further difference between these two tasks is that while yes/no detection is a subjective task, which is affected by a decision bias, 2IFC detection is an objective, bias-free, task (Azzopardi and Cowey, 1997). However, since cardiac phase was found to mainly affect the sensitivity aspect of detection, it is not likely that the objectivity of the 2IFC task hindered the cardiac phase effects on it.

Another interpretation of these cardiac phase-dependent effects can be systematic changes in peripheral noise levels across the cardiac cycle, which can potentially be transmitted to central neural structures (Galvez-Pol et al., 2020; Ohl et al., 2016). During systole, an increase in physiological noise can decrease the signal-to-noise ratio for the processing of external stimuli. While this noise modulation is probably happening and might contribute to the observed findings, it does not fully explain how the pulse-related neural changes themselves are attenuated from conscious perception such that we don't continuously feel the heartbeat-related sensations. For this to happen, central suppression via a predictive model might play a role. The existence of such predictive models has been shown also for other modalities. For example, is has been shown that the processing of heartbeat-coupled sounds are attenuated, which suggests the existence of predictive mechanisms to suppress stimuli concurrent with bodily signals (Van Elk et al., 2014). Supporting the involvement of central predictive mechanisms, we found that only a late component of the SEPs, the P300, was weaker during systole. Increased noise in the peripheral receptors are likely to affect also earlier SEP components such as the P50, which reflects mainly activity in SI (Allison et al., 1989), and the N140, both of which have been shown to be sensitive to bottom-up effects (Forschack et al., 2020). Thus, the effect of cardiac phase on late somatosensory neural processing is consistent with a top-down central mechanism, which should be explicitly tested in future studies.

A significant difference in the P300 component was observed between 512 and 600 ms after the stimulation, which was later than the 268–468 ms window that was observed in our earlier study (Al et al., 2020). One reason could be "statistical" in nature: Perhaps the entire P300 is more pronounced in diastole, but with the limited sample sizes, the effect on the first window (268–468) stayed only as a trend in the current study ($p = 0.07$). Another speculative explanation relates to the different stimulation paradigms in the two studies: While in our previous study subjects expected a stimulus on either the left index or middle finger at a certain stimulation interval, in the current experiment, subjects received a stimulation on the left index finger in one of the two stimulation intervals. Therefore, subjects had a higher spatial but lower temporal certainty about the stimulation in the current study. As stimulation expectancy can influence late evoked activity (Auksztulewicz et al., 2018), this experimental modulation might be responsible for changes in the latency of the cardiac effect on P300 amplitude.

We previously suggested that this change in P300 amplitude can be associated with a more accurate prediction of the pulse-wave (as a result of a smaller 'prediction error') (Al et al., 2020; Friston, 2005). Despite the different time windows in which the effect was statistically significant, current results support the notion that the weaker P300 amplitude during systole is a result of perceptual suppression of the peripheral activity via central prediction (Al et al., 2020). The smaller P300 amplitude during systole might indicate a less efficient propagation of somatosensory information to higher cortical areas (Vugt et al., 2018). Such a decrease in neural propagation could interfere with both the global broadcasting of the stimulus (Dehaene et al., 2003) and/or late recurrent activity within somatosensory areas (Auksztulewicz et al., 2012; Lamme, 2006), both of which can suppress the conscious perception of the external stimulus.

Cardiac phase effects were also investigated depending on the stimulation interval. While the interval was not observed to significantly interact with the cardiac phase effects, it influenced stimulus detection. Specifically, when a stimulus was presented in the second compared to the first temporal interval, it was detected more often. This increase in detection went along with higher P300 amplitudes during the second interval. The increased detection and P300 amplitudes might be related to an increased temporal certainty of a stimulus presentation during the second interval following no stimulation in the first interval. Therefore, it is likely that subjects had higher temporal *attention* to the stimuli during the second interval. We also investigated whether the effect of stimulation interval on P300 interacted with the cardiac phase. While the raw comparisons (Fig. 2) seem to indicate that P300 amplitude differences might only be present during the first interval (which could be due to ceiling effects in the second interval), importantly, no significant interaction effect was found between interval and cardiac phase, i.e., a difference of cardiac effects on detection or P300 between the two intervals cannot be claimed based on our data.

In addition to detection and P300 amplitudes, the effect of stimulation interval was also investigated on heart rate. Interestingly, stimulation during the first interval was accompanied by a cardiac acceleration. Since the prestimulus window was short in the experiment, this acceleration might be related to a post-stimulation effect from the previous trial, particularly from the motor response. When the stimulation was presented not in the first but in the second interval, a cardiac deceleration was observed, as would be expected with somatosensory stimulation (Motyka et al., 2019). While the comparison of pre-stimulus heartbeat changes between the two temporal windows is probably "contaminated" by the effects of the last trial, the temporal certainty about the stimulation during the second interval most likely contributes to the increase in interbeat interval length, possibly driven by a rapid parasympathetic response to stimulation. This might facilitate stimulus detection during the second interval as the cardiac deceleration is known to be associated with increased somatosensory detection (Motyka et al., 2019).

Similar to the cardiac phase, the amplitude of prestimulus HEP also affected somatosensory processing. Here, we replicated the finding of higher HEP amplitudes between 296 and 400 ms, over centroparietal electrodes, being followed by decreased somatosensory detection. This decrease in somatosensory detection was related to a more conservative detection bias (criterion). Since a conservative bias is known to relate to lower baseline firing rate in the brain, higher amplitudes of HEP might interfere with upcoming stimulus detection by preventing the early neuronal activity from reaching the threshold of 'ignition' (according to global neuronal workspace theory) (Dehaene and Changeux, 2011; Vugt et al., 2018). In line with this argument, we confirmed the interference of higher HEP amplitudes with both early (P50) and later (N140, P300) SEP amplitudes in the sensory level. Following the higher prestimulus HEP amplitudes we also observed significant changes of the source-localized P50 amplitude in the contralateral somatosensory cortex, right insular cortex, lateral prefrontal cortex, and posterior cingulate cortex. Among these regions, the right anterior insula is known to play a crucial role in regulating attention, internally and externally, possibly through its connections with the lateral prefrontal cortex and posterior cingulate cortex, which are also associated with attentional control (Critchley et al., 2004; Leech and Sharp, 2014). Since HEP amplitudes have been previously demonstrated to be higher when attention is directed internally compared to externally (García-Cordero et al., 2017; Petzschner et al., 2019; Villena-González et al., 2017), we reiterate our earlier interpretation that increases in HEP amplitudes preceding misses indicate a shift in attention from external stimuli to internal bodily signals (Al et al., al.,2020).

Supporting the interpretation of the increased HEP levels resulting from attention being oriented internally, we found that subjects had higher HEP amplitudes when they were resting compared to engaging in a somatosensory task. In sensory level, HEPs during the resting state were found to be higher than those preceding hits, but not misses. In other words, subjects' HEP amplitudes preceding misses, during the somatosensory task, were similar to their level during the resting-state, when exteroceptive attention is expected to be minimal. Thus, these re-

sults further substantiate increases in HEP amplitudes reflecting a state of mind focused on interoceptive relative to exteroceptive processes, which interferes with conscious somatosensory detection. One specific reason why the somatosensory system might be particularly sensitive to modulations of interoception, might be the fact that both interoception and somatosensation rely on processes in the primary somatosensory cortex (Critchley et al., 2004; Khalsa et al., 2009; Pollatos et al., 2007). For example, somatosensory sensations on the chest have been shown to contribute to interoceptive awareness (Khalsa et al., 2009; Knapp-Kline, Ring, Emmerich, and Brener, 2021). While in our study, the somatosensory stimuli were not applied to the chest but to the finger, future studies can investigate whether somatosensory stimulation of the chest would amplify the interference of interoceptive processes with exteroception.

Source analysis of HEP fluctuations related to detection versus misses of somatosensory stimuli revealed two regional clusters. The first extended from the right postcentral gyrus and sulcus and the paracentral lobule and sulcus to the superior parietal lobule. The other extended across the right precuneus, isthmus of the cingulate, middle and posterior cingulate cortex, and the pericallosal sulcus (see **Fig. 4**). Furthermore, in these regions, HEP levels preceding misses were near the level of those during a resting-state condition. Among these regions, the postcentral gyrus, the paracentral lobule, middle and posterior cingulate cortex, and precuneus have been previously found to show higher activity during interoception compared to exteroception and to correlate with interoceptive awareness (Stern et al., 2017). Interestingly, a strong functional connection of the precuneus and posterior cingulate cortex with sensorimotor areas including the superior parietal lobule, paracentral lobule, and postcentral gyrus has been observed previously (Margulies et al., 2009; Morecraft et al., 2004; Nierhaus et al., 2015; Vogt and Vogt, 2003). Furthermore, the precuneus and posterior cingulate cortex are important parts of the default mode network (DMN) (Fransson and Marrelec, 2008; Raichle et al., 2001). The DMN shows higher activation during resting conditions relative to external attention-demanding tasks and has been linked to self-referential mental activity and interoception (Buckner et al., 2008; Kleckner et al., 2017). Taken together, these results provide a plausible neural basis for the interpretation that higher HEP amplitudes reflect a state of mind focused on internal processes.

As a limitation of our study, it is important to mention that the HEP analyses included only stimuli that occurred during diastole. This is due to the fact that the HEP occurs during the systolic time window, i.e., any stimulation during this time window could “contaminate” the HEP signal. This implies that the strength of cortical processing of the heartbeat, indexed by HEPs - recorded during systole - affects detection of following somatosensory stimuli during diastole.

This point touches the important question about the overall idea how to conceptionally integrate the two different heartbeat-related effects (phase, HEP) which we report here. Our current interpretation is that they reflect two fundamental neuro-cognitive processes related to cardiac function, i.e., prediction (phase) and attention (HEP). While it is likely that these processes are also interrelated, the underlying neural mechanisms are mostly unknown. What follows are some speculative considerations: The brain is quickly (and pre-attentively) informed about each heartbeat e.g., by baroreceptors. We assume that the HEP reflects the cortical processing of this bottom-up information about the heartbeat. Neural origins underlying the HEP have been shown – among others - in the insula as well as primary and secondary somatosensory cortices (Kern et al., 2013; Park et al., 2018; Pollatos et al., 2005). It is thus tempting to suggest that neural (HEP) processing in SII and insula, areas known to encode prediction of somatosensory stimulation (Andersen and Lundqvist, 2019), could reflect the predictive aspect leading to suppression of external somatosensory stimuli in systole. Processing of HEP in other areas e.g., those for which we noted HEP-differences between hits and misses (right parietal and cingulate areas) might reflect the shifts between interoceptive versus exteroceptive attention. Future studies will have to clarify the contribution of these brain areas to heart-brain interactions.

In summary, this study confirms the two different effects of cardiac phase and HEP amplitudes on somatosensory perception and evoked potentials. We interpret the cardiac phase effects in an interoceptive predictive coding framework and link the HEP effects with spontaneous switches between interoceptive and exteroceptive attention. Our additional finding that HEP during the task is smaller than during resting state further supports the latter interpretation. Lastly, a new source analysis of HEP fluctuation provides a neural underpinning for the switch between interoception and exteroception.

Data and code availability

Data and code will be available upon request. Due to a lack of explicit consent on the part of the participants to data sharing, structural MRI and EEG data cannot be shared publicly. Such data can only be shared upon request if data privacy can be guaranteed according to the rules of the European General Data Protection Regulation (EU GDPR).

Declaration of Competing Interest

The authors declare no competing financial interests.

Credit authorship contribution statement

Esra Al: Conceptualization, Data curation, Formal analysis, Investigation, Methodology, Project administration, Software, Validation, Visualization, Writing – original draft, Writing – review & editing. **Fivos Iliopoulos:** Conceptualization, Data curation, Software. **Vadim V. Nikulin:** Conceptualization, Methodology, Writing – review & editing. **Arno Villringer:** Conceptualization, Funding acquisition, Investigation, Methodology, Project administration, Resources, Supervision, Validation, Writing – review & editing.

Acknowledgments

We thank Sylvia Stasch for technical assistance with data acquisition, Eleni Panagoulas for helping with data preprocessing, Dan John Cook and Joshua Grant for their valuable comments on the manuscript.

Supplementary materials

Supplementary material associated with this article can be found, in the online version, at doi:10.1016/j.neuroimage.2021.118247.

References

Al, E., Iliopoulos, F., Forschack, N., Nierhaus, T., Grund, M., Motyka, P., …, Villringer, A., 2020. Heart-brain interactions shape somatosensory perception and evoked potentials. Proc. Natl. Acad. Sci. U.S.A. 117 (19), 10575–10584. doi:10.1073/pnas.1915629117.

Allison, T., McCarthy, G., Wood, C.C., Darcey, T.M., Spencer, D.D., Williamson, P.D., 1989. Human cortical potentials evoked by stimulation of the median nerve. I. Cytoarchitectonic areas generating short-latency activity. J. Neurophysiol. 62 (3), 694–710. doi:10.1152/jn.1989.62.3.694.

Andersen, L.M., Lundqvist, D., 2019. Somatosensory responses to nothing: an MEG study of expectations during omission of tactile stimulations. Neuroimage 184, 78–89. doi:10.1016/j.neuroimage.2018.09.014.

Auksztulewicz, R., Schwiedrzik, C.M., Thesen, T., Doyle, W., Devinsky, O., Nobre, A.C., …, Melloni, L., 2018. Not all predictions are equal: “what” and “when” predictions modulate activity in auditory cortex through different mechanisms. J. Neurosci. 38 (40), 8680–8693. doi:10.1523/JNEUROSCI.0369-18.2018.

Auksztulewicz, R., Spitzer, B., Blankenburg, F., 2012. Recurrent neural processing and somatosensory awareness. J. Neurosci. 32 (3), 799–805.

Azzopardi, P., Cowey, A., 1997. Is blindsight like normal, near-threshold vision? Psychology 94, 14190–14194.

Barrett, L.F., Simmons, W.K., 2015. Interoceptive predictions in the brain. Nat. Rev. Neurosci. 16 (7), 419–429. doi:10.1038/nrn3950.

Buckner, R.L., Andrews-Hanna, J.R., Schacter, D.L., 2008. The brain’s default network: anatomy, function, and relevance to disease. Ann. N. Y. Acad. Sci. doi:10.1196/annals.1440.011, Ann N Y Acad Sci.

Chaumon, M., Bishop, D.V.M., Busch, N.A, 2015. A practical guide to the selection of independent components of the electroencephalogram for artifact correction. J. Neurosci. Methods 250, 47–63. doi:10.1016/j.jneumeth.2015.02.025.
Critchley, H.D., Garfinkel, S.N., 2018. The influence of physiological signals on cognition. Curr. Opin. Behav. Sci. 19, 13–18. doi:10.1016/j.cobeha.2017.08.014.
Critchley, H.D., Wiens, S., Rotshtein, P., Öhman, A., Dolan, R.J., 2004. Neural systems supporting interoceptive awareness. Nat. Neurosci. 7 (2), 189–195. doi:10.1038/nn1176.
Dehaene, S., Changeux, J.-.P., 2011. Experimental and theoretical approaches to conscious processing. Neuron 70 (2), 200–227.
Dehaene, S., Sergent, C., Changeux, J.-.P., 2003. A neuronal network model linking subjective reports and objective physiological data during conscious perception. Proc. Natl. Acad. Sci. 100 (14), 8520–8525. doi:10.1073/pnas.1332574100.
Delorme, A., Makeig, S., 2004. EEGLAB: an open source toolbox for analysis of single-trial EEG dynamics including independent component analysis. J. Neurosci. Methods doi:10.1016/j.jneumeth.2003.10.009.
Delorme, A., Palmer, J., Onton, J., Oostenveld, R., Makeig, S., 2012. Independent EEG sources are dipolar. PLoS One 7 (2), e30135. doi:10.1371/journal.pone.0030135.
Destrieux, C., Fischl, B., Dale, A., Halgren, E., 2010. Automatic parcellation of human cortical gyri and sulci using standard anatomical nomenclature. Neuroimage 53 (1), 1–15. doi:10.1016/j.neuroimage.2010.06.010.
Edwards, L., Ring, C., Mcintyre, D., Winer, J., Martin, U., 2009. Sensory detection thresholds are modulated across the cardiac cycle: evidence that cutaneous sensibility is greatest for systolic stimulation. Psychophysiology 46, 252–256. doi:10.1111/j.1469-8986.2008.00769.x.
Fonov, V., Evans, A., McKinstry, R., Almli, C., Collins, D., 2009. Unbiased nonlinear average age-appropriate brain templates from birth to adulthood. Neuroimage 47, S102. doi:10.1016/s1053-8119(09)70884-5.
Forschack, N., Nierhaus, T., Müller, M.M., Villringer, A., 2020. Dissociable neural correlates of stimulation intensity and detection in somatosensation. Neuroimage 217. doi:10.1016/j.neuroimage.2020.116908.
Fransson, P., Marrelec, G., 2008. The precuneus/posterior cingulate cortex plays a pivotal role in the default mode network: evidence from a partial correlation network analysis. Neuroimage 42 (3), 1178–1184. doi:10.1016/j.neuroimage.2008.05.059.
Friston, K., 2005. A theory of cortical responses. Philos. Trans. R. Soc. B Biol. Sci. 360 (1456), 815–836. doi:10.1098/rstb.2005.1622.
Galvez-Pol, A., McConnell, R., Kilner, J.M., 2020. Active sampling in visual search is coupled to the cardiac cycle. Cognition 196. doi:10.1016/j.cognition.2019.104149.
García-Cordero, I., Esteves, S., Mikulan, E.P., Hesse, E., Baglivo, F.H., Silva, W., …, Sedeño, L., 2017. Attention, in and out: scalp-level and intracranial EEG correlates of interoception and exteroception. Front. Neurosci. 11, 411. doi:10.3389/fnins.2017.00411.
Garfinkel, S.N., Minati, L., Gray, M.A., Seth, A.K., Dolan, R.J., Critchley, H.D., 2014. Fear from the heart: sensitivity to fear stimuli depends on individual heartbeats. J. Neurosci. 34 (19), 6573–6582. doi:10.1523/JNEUROSCI.3507-13.2014.
Gramfort, A., Papadopoulo, T., Olivi, E., Clerc, M., 2010. OpenMEEG: opensource software for quasistatic bioelectromagnetics. Biomed. Eng. Online 9 (1), 45. doi:10.1186/1475-925X-9-45.
Gray, M.A., Minati, L., Paoletti, G., Critchley, H.D., 2010. Baroreceptor activation attenuates attentional effects on pain-evoked potentials. Pain 151 (3), 853–861. doi:10.1016/j.pain.2010.09.028.
Kern, M., Aertsen, A., Schulze-Bonhage, A., Ball, T., 2013. Heart cycle-related effects on event-related potentials, spectral power changes, and connectivity patterns in the human ECoG. Neuroimage 81, 178–190. doi:10.1016/J.NEUROIMAGE.2013.05.042.
Khalsa, S.S., Rudrauf, D., Feinstein, J.S., Tranel, D., 2009. The pathways of interoceptive awareness. Nat. Neurosci. 12 (12), 1494–1496. doi:10.1038/nn.2411.
Kleckner, I.R., Zhang, J., Touroutoglou, A., Chanes, L., Xia, C., Simmons, W.K., …, Feldman Barrett, L., 2017. Evidence for a large-scale brain system supporting allostasis and interoception in humans. Nat. Hum. Behav. 1, 69. doi:10.1038/s41562-017-0069.
Knapp-Kline, K., Ring, C., Emmerich, D., Brener, J., 2021. The effects of vibrotactile masking on heartbeat detection: evidence that somatosensory mechanoreceptors transduce heartbeat sensations. Psychophysiology e13817. doi:10.1111/psyp.13817.
Kybic, J., Clerc, M., Abboud, T., Faugeras, O., Keriven, R., Papadopoulo, T., 2005. A common formalism for the Integral formulations of the forward EEG problem. IEEE Trans. Med. Imaging 24 (1), 12–28. doi:10.1109/TMI.2004.837363.
Lamme, V.A.F, 2006. Towards a true neural stance on consciousness. Trends Cognit. Sci. (Regul. Ed.) 10 (11), 494–501. doi:10.1016/J.TICS.2006.09.001.
Leech, R., Sharp, D.J., 2014. The role of the posterior cingulate cortex in cognition and disease. Brain doi:10.1093/brain/awt162, Oxford University Press.
Macefield, V.G., 2003. Cardiovascular and respiratory modulation of tactile afferents in the human finger pad. Exp. Physiol. 88 (5), 617–625. Retrieved from http://www.ncbi.nlm.nih.gov/pubmed/12955162 .
Margulies, D.S., Vincent, J.L., Kelly, C., Lohmann, G., Uddin, L.Q., Biswal, B.B., …, Petrides, M., 2009. Precuneus shares intrinsic functional architecture in humans and monkeys. Proc. Natl. Acad. Sci. U.S.A. 106 (47), 20069–20074. doi:10.1073/pnas.0905314106.
Marshall, A.C., Gentsch, A., Jelinčić, V., Schütz-Bosbach, S., 2017. Exteroceptive expectations modulate interoceptive processing: repetition-suppression effects for visual and heartbeat evoked potentials. Sci. Rep. 7 (1), 1–15. doi:10.1038/s41598-017-16595-9.
Marshall, A.C., Gentsch, A., Schröder, L., Schütz-Bosbach, S., 2018. Cardiac interoceptive learning is modulated by emotional valence perceived from facial expressions. Soc. Cognit. Affect. Neurosci. 13 (7), 677–686. doi:10.1093/scan/nsy042.
Morecraft, R.J., Cipolloni, P.B., Stilwell-Morecraft, K.S., Gedney, M.T., Pandya, D.N., 2004. Cytoarchitecture and cortical connections of the posterior cingulate and adjacent somatosensory fields in the rhesus monkey. J. Comp. Neurol. 469 (1), 37–69. doi:10.1002/cne.10980.
Motyka, P., Grund, M., Forschack, N., Al, E., Villringer, A., Gaebler, M., 2019. Interactions between cardiac activity and conscious somatosensory perception. Psychophysiology e13424.
Nierhaus, T., Forschack, N., Piper, S.K., Holtze, S., Krause, T., Taskin, B., …, Villringer, A., 2015. Imperceptible somatosensory stimulation alters sensorimotor background rhythm and connectivity. J. Neurosci. 35 (15), 5917–5925.
Ohl, S., Wohltat, C., Kliegl, R., Pollatos, O., Engbert, R., 2016. Microsaccades are coupled to heartbeat. J. Neurosci. 36 (4), 1237–1241. doi:10.1523/JNEUROSCI.2211-15.2016.
Oostenveld, R., Fries, P., Maris, E., Schoffelen, J.-.M., 2011. FieldTrip: open source software for advanced analysis of MEG, EEG, and invasive electrophysiological data. Comput. Intell. Neurosci. 2011, 1–9. doi:10.1155/2011/156869.
Park, H.D., Bernasconi, F., Salomon, R., Tallon-Baudry, C., Spinelli, L., Seeck, M., …, Blanke, O., 2018. Neural sources and underlying mechanisms of neural responses to heartbeats, and their role in bodily self-consciousness: an intracranial EEG study. Cereb. Cortex 28 (7), 2351–2364. doi:10.1093/cercor/bhx136.
Perakakis, P. (2019). HEPLAB: a Matlab graphical interface for the preprocessing of the heartbeat-evoked potential. 10.5281/ZENODO.2649943
Petzschner, F.H., Weber, L.A., Wellstein, K.V., Paolini, G., Do, C.T., Stephan, K.E., 2019. Focus of attention modulates the heartbeat evoked potential. Neuroimage 186, 595–606. doi:10.1016/J.NEUROIMAGE.2018.11.037.
Pollatos, O., Kirsch, W., Schandry, R., 2005. Brain structures involved in interoceptive awareness and cardioafferent signal processing: a dipole source localization study. Hum. Brain Mapp. 26 (1), 54–64. doi:10.1002/hbm.20121.
Pollatos, O., Schandry, R., Auer, D.P., Kaufmann, C., 2007. Brain structures mediating cardiovascular arousal and interoceptive awareness. Brain Res. 1141 (1), 178–187. doi:10.1016/j.brainres.2007.01.026.
Raichle, M.E., MacLeod, A.M., Snyder, A.Z., Powers, W.J., Gusnard, D.A., Shulman, G.L., 2001. A default mode of brain function. In: Proceedings of the National Academy of Sciences of the United States of America, 98, pp. 676–682. doi:10.1073/pnas.98.2.676.
Sandman, C.A., McCanne, T.R., Kaiser, D.N., Diamond, B., 1977. Heart rate and cardiac phase influences on visual perception. J. Comp. Physiol. Psychol. 91 (1), 189–202. doi:10.1037/h0077302.
Saxon, S.A., 1970. Detection of near threshold signals during four phases of cardiac cycle. Ala. J. Med. Sci. 7 (4), 427–430. Retrieved from http://www.ncbi.nlm.nih.gov/pubmed/5532273 .
Schandry, R., Sparrer, B., Weitkunat, R., 1986. From the heart to the brain: a study of heartbeat contingent scalp potentials. Int. J. Neurosci. 30 (4), 261–275. Retrieved from http://www.ncbi.nlm.nih.gov/pubmed/3793380 .
Schandry, R., Weitkunat, R., 1990. Enhancement of heartbeat-related brain potentials through cardiac awareness training. Int. J. Neurosci. 53 (2–4), 243–253. Retrieved from http://www.ncbi.nlm.nih.gov/pubmed/2265945 .
Seth, A.K., Friston, K.J., 2016. Active interoceptive inference and the emotional brain. Philos. Trans. R. Soc. B Biol. Sci. (1708) 371. doi:10.1098/rstb.2016.0007.
Stern, E.R., Grimaldi, S.J., Muratore, A., Murrough, J., Leibu, E., Fleysher, L., …, Burdick, K.E., 2017. Neural correlates of interoception: effects of interoceptive focus and relationship to dimensional measures of body awareness. Hum. Brain Mapp. 38 (12), 6068–6082. doi:10.1002/hbm.23811.
Tadel, F., Baillet, S., Mosher, J.C., Pantazis, D., Leahy, R.M., 2011. Brainstorm: a user-friendly application for MEG/EEG analysis. Comput. Intell. Neurosci. 2011. doi:10.1155/2011/879716.
Van Elk, M., Lenggenhager, B., Heydrich, L., Blanke, O., 2014. Suppression of the auditory N1-component for heartbeat-related sounds reflects interoceptive predictive coding. Biol. Psychol. 99 (1), 172–182. doi:10.1016/j.biopsycho.2014.03.004.
Vázquez-Seisdedos, C.R., Neto, J.E., Marañón Reyes, E.J., Klautau, A., Limão de Oliveira, R.C., 2011. New approach for T-wave end detection on electrocardiogram: performance in noisy conditions. Biomed. Eng. Online 10, 77. doi:10.1186/1475-925X-10-77.
Villena-González, M., Moënne-Loccoz, C., Lagos, R.A., Alliende, L.M., Billeke, P., Aboitiz, F., …, Cosmelli, D., 2017. Attending to the heart is associated with posterior alpha band increase and a reduction in sensitivity to concurrent visual stimuli. Psychophysiology 54 (10), 1483–1497. doi:10.1111/psyp.12894.
Vogt, B.A., Vogt, L., 2003. Cytology of human dorsal midcingulate and supplementary motor cortices. J. Chem. Neuroanat. 26, 301–309. doi:10.1016/j.jchemneu.2003.09.004.
Vugt, B.V., Dagnino, B., Vartak, D., Safaai, H., Panzeri, S., Dehaene, S., Roelfsema, P.R., 2018. The threshold for conscious report: signal loss and response bias in visual and frontal cortex. Science 360 (6388), 537–542. doi:10.1126/SCIENCE.AAR7186.
Wilkinson, M., McIntyre, D., Edwards, L., 2013. Electrocutaneous pain thresholds are higher during systole than diastole. Biol. Psychol. 94 (1), 71–73. doi:10.1016/j.biopsycho.2013.05.002.
Zhang, Y., Ding, M., 2010. Detection of a weak somatosensory stimulus: role of the Prestimulus Mu rhythm and its top–down modulation. J. Cognit. Neurosci. 22 (2), 307–322. doi:10.1162/jocn.2009.21247.